Structural investigations of human hairs by spectrally resolved ellipsometry

Danny Chan
Benjamin Schulz
Michael Rübhausen
Universität Hamburg
Institut für Angewandte Physik
Hamburg, Germany

Sonja Wessel
Roger Wepf
Beiersdorf AG
Hamburg, Germany

Abstract. Human hair is a biological layered system composed of two major layers, the cortex and the cuticle. We show spectrally resolved ellipsometry measurements of the ellipsometric parameters Ψ and Δ of single human hairs. The spectra reflect the layered nature of hair and the optical anisotropy of the hair's structure. In addition, measurements on strands of human hair show a high reproducibility of the ellipsometric parameters for different hair fiber bundles from the same person. Based on the measurements, we describe a dielectric model of hair that explains the spectra in terms of the dielectric properties of the major parts of hair and their associated layer thicknesses. In addition, surface roughness effects modeled by a roughness layer with a complex refractive index given by an effective medium approach can be seen to have a significant effect on the measurements. We derive values for the parameters of the cuticle surface roughness layer of the thickness $d_{ACu}=273$ to 360 nm and the air inclusion $f_A=0.6$ to 5.7%.
[DOI: 10.1117/1.2162848]

Keywords: human hair; ellipsometry; modeling; spectra.

Paper 05068 received Mar. 17, 2005; accepted for publication Jul. 4, 2005; published online Jan. 24, 2006.

1 Introduction

Human hair is an example of a layered bio-organic dead material. Hairs are appendages of skin with circular or elliptical cross sections and typical diameters of about 70 μm.[1] They consist of two major layers, the cuticle and the cortex. The cortex forms the so-called hair shaft and is comprised of long cornified cells with lengths of about 100 μm, which are oriented along the hair axis and embedded in the cell membrane complex. The cortex consists mainly of α-keratin and is also the location for the hair pigment melanin, which gives hairs their specific color. The cuticle in contrast consists of four to eight layers of overlapping cornified keratin-filled cells with thicknesses of roughly 350 to 500 nm, forming a protective layer of 1 to 3 μm thickness on top of the cortex.[1,2] Each cell itself is further divided into several sublayers.[1] The visual appearance of hairs is often said to be closely linked to the state of the cuticle.

Investigations of the structural parameters of human hair are important for cosmetic applications. In addition, hairs as an exemplary biological layered system are ideal for studying the applicability of theoretical models for the description of ellipsometric measurements.

Measurements of the structural parameters of hairs are often made using electron microscopy or optical microscopy. However, since these techniques are limited to single hair measurements, the number of samples for a study is rather small.

In addition, goniophotometric techniques have been employed for measurement of structural parameters of the cuticle, such as the mean angle of the cuticle cells to the cortex or the surface roughness. Again, for single hair measurements, sample throughput is not adequate for a good statistical analysis. Moreover, simultaneous measurements on hair collections is possible, but requires careful preparation of the hairs in a row of perfectly aligned hairs. This makes goniophotometric methods unsuitable for screening a large number of samples.[3,4]

We present measurements of the wavelength-dependent ellipsometric parameters Ψ and Δ of human hairs. Measurements of single hairs in two geometries are shown as well as measurements on strands of hairs with the hairs oriented parallel to the plane of incidence. We show that ellipsometry is able to resolve the optical anisotropy and the layered structure of human hair. A simple dielectric model accounting for the layered structure of hair and the interface roughnesses between the layers is able to describe the data of the measurements on hair strands qualitatively well.

2 Experimental Details

Ellipsometry is an optical technique that analyzes the change in polarization of a light beam on reflection on the sample surface.[5] It can establish optical and structural parameters of complex layered systems with high accuracy while working with low power densities in the probe beam that hardly influence the samples. In contrast to methods measuring the total reflection or transmission of light, ellipsometry measures two

Address all correspondence to Benjamin Schulz, Institut für Angewandte Physik, Jungiusstraße 11, Hamburg, Hamburg 20355, Germany. Tel: +49–40–428384202. Fax: +49–40–42838–4368. E-mail: ben99@gmx.net

1083-3668/2006/11(1)/014029/6/$22.00 © 2006 SPIE

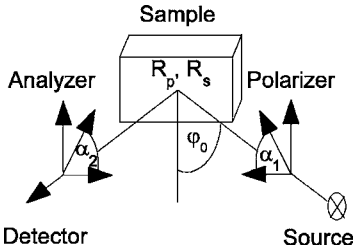

Fig. 1 Principle of ellipsometry. Light emitted by a light source, which may be a laser or a broadband source. It is polarized and reflected by the sample under an angle ϕ_0. The beam is analyzed by a rotating analyzer and the detector.

parameters simultaneously, the ellipsometric parameters Ψ and Δ.

In ellipsometry, linear or circular polarized light is reflected by the sample under an angle ϕ_0. The change in polarization on reflection is analyzed using a rotating polarizer (see Fig. 1).

The measured intensity changes are converted to the ellipsometric parameters Ψ and Δ. These parameters signify the change in polarization due to the refractive index mismatch between different structural features of the system, and are restricted to the range 0 to 360 deg. They are calculated using only intensity ratios measured at different analyzer angles. Therefore, this technique is self-normalizing, which results in its high accuracy. The basic equation for ellipsometry is

$$\rho = \tan(\Psi)\exp(i\Delta) = \frac{R_p}{R_s}, \tag{1}$$

where R_p and R_s are the complex reflection coefficients for the components of the light being parallel and perpendicular to the plane of incidence, respectively. Since R_p and R_s depend on structural as well as dielectric properties of the sample, the resulting expression can become very complex. Usually, the resulting equation is nonlinear and transcendent and cannot, therefore, analytically be inverted to yield the parameters of interest like complex refractive indices, layer thicknesses, etc.[5]

In the case of a homogeneous, isotropic, and within the penetration depth infinitely thick sample, the complex reflection coefficients are the well known Fresnel parameters. Only in the case of a so-called bulk system, the ellipsometric parameters Ψ and Δ can be analytically converted to the complex refractive index N_1 of the sample by

$$N_1 = N_0 \tan\phi_0 \left[1 - \frac{4\rho}{(1+\rho)^2}\sin^2\phi_0\right]^{1/2}, \tag{2}$$

where N_0 is the complex refractive index of the ambient, which is usually air and can be set in good approximation to 1.

For stratified systems with $n+1$ layers, where each layer is homogeneous and isotropic, a 2×2 matrix formalism can be used to compute an expression for R_p/R_s. In this case, a scattering matrix $\mathbf{S}$ is computed by

$$\mathbf{S}_{s,p} = \mathbf{I}_{01s,p}\mathbf{L}_1\mathbf{I}_{12s,p}\mathbf{L}_2 \ldots \mathbf{L}_n\mathbf{I}_{n(n+1)s,p}. \tag{3}$$

Here, the matrices $\mathbf{I}_{m(m+1)s,p}$ describe the influence of an interface between two layers m and $m+1$ and depend, therefore, on the Fresnel coefficients of the interface. The layer matrix $\mathbf{L}_m$, on the other hand, describes the phase shift of the polarization of the light beam due to the distance traveled within the layer m and depends on the thickness, the local angle of incidence, and the complex refractive index of the layer.

The ratio of the complex reflection coefficients R_p/R_s needed to analyze Eq. (1) can then be calculated to be

$$\frac{R_p}{R_s} = \frac{S_{21p}}{S_{11p}} \cdot \frac{S_{11s}}{S_{21s}}. \tag{4}$$

The effect of surface roughnesses on the polarization can be modeled by use of the effective medium approximation. The effective medium approximation describes the influence of a host medium with complex refractive index N_h, in which small spheres with complex refractive index N_b are embedded, by an effective complex refractive index N_e, given by

$$\frac{N_e^2 - N_h^2}{N_e^2 + 2N_h^2} = f\frac{N_b^2 - N_h^2}{N_b^2 + 2N_h^2}, \tag{5}$$

where f is the volume fraction of the embedded material. Interface roughnesses between two layers can then be modeled by replacing the surface roughness with a roughness layer, where its refractive index is given by an effective medium composed of the two materials of the adjacent layers.[5]

All measurements were performed on a Sentech SE850 spectrally resolving ellipsometer. The wavelength range investigated in the measurements was 330 to 790 nm.

The single hair measurements were performed using focusing units. These focusing units focus down the beam from a diameter of about 6 mm down to a diameter of about 200 μm. Since the focusing units work with dispersive lenses, systematic errors due to chromatic aberrations can occur. Also, when using the focusing probes, the angle of incidence has to be integrated over the aperture angle of the lenses. Test measurements on silicon wafers, however, show that the resulting error can be estimated to be less than 10^{-2} in n and k for our lenses with a small numerical aperture, and therefore are weak focusing.[6]

The single hair measurements were performed on European blond hair. Up to ten positions were measured on ten different hairs. Measurements on single hairs were performed with the hair oriented parallel and perpendicular with respect to the plane of incidence to check for optical anisotropy. The hairs were measured on a sample holder consisting of several pieces of sandblasted silicon arranged in a bridge-like fashion, so that the hair is several millimeters elevated above the silicon. This ensures that no back reflex from the silicon can enter the detector. Samples were fixated onto the holder using double-sided adhesive tape. The required time for one measurement was $\approx$3 min.

The measurements on hair strands were performed using a custom-made sample holder. The holder fixates the hair strands several centimeters elevated above the sample holder, similar to the sample holder for the single hair measurements. No attempt was made to order all hairs perfectly parallel. All

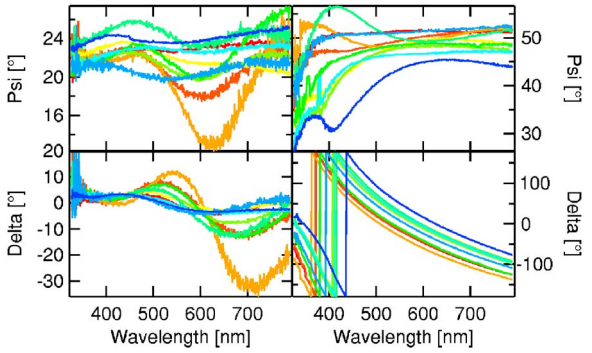

Fig. 2 Single hair measurements on ten positions along an European blond hair. Left: hair oriented parallel to the plane of incidence. Right: hair oriented perpendicular to the plane of incidence. Values of Δ in the range $180\ \text{deg} \leqslant \Delta \leqslant 360\ \text{deg}$ are mapped to the range -180 to 0 deg for better visibility of the zero crossings in the parallel orientation.

measurements were performed without the microfocusing option, thereby resulting in a measurement spot on the sample of about 2×7 cm. Due to intensity restrictions, only measurements in the parallel configuration were possible. The required time for one measurement was 3 to 5 min.

3 Results

Figure 2 shows spectra of the ellipsometric parameters Ψ and Δ of a European blond single hair at ten different positions along the hair. The hair was measured with the hair oriented parallel and perpendicular to the plane of incidence. A clear anisotropy can be seen in the spectra for the two orientations. This optical anisotropy reflects the natural growth direction of hair with its strongly directed keratin filaments in the cortex. Also, in both orientations, zero crossings in the parameter Δ are visible. This is a clear indication for the existence of a layered system, since in a bulk system the value of Δ is confined to the range $0\ \text{deg} \leqslant \Delta \leqslant 180\ \text{deg}$, as can be readily seen in Eq. (2).

The measurements show large variations in the values of the ellipsometric parameters and the shape of the spectra. This is due to the local variation in chemical composition and the difference in the morphological features, especially the cuticle thickness and the surface roughness. In particular, the variation in the surface structure can have a significant effect on the ellipsometric spectra. These variations in the chemical composition and the morphological structure are even visible in a single hair, since hairs can have experienced very different environments, treatment, mechanical wear, etc., depending on the position and therefore the age of the spot along the hair.

To reduce the variation in the ellipsometric parameters in the single hair measurements, a setup for measuring strands of hairs was established. The simultaneous measurement of a large collection of hairs leads to more reproducible results. Furthermore, the strong condition by the detector accepted angle of reflection results in a technique that is not sensitive to the arrangement of the single hairs in the strand.

For the measurements, 12 hair strands from six different persons were measured, making a total of two samples for each person. Each sample was measured at ten positions. Figure 3 shows the results of these measurements.

For all samples, a good reproducibility of the spectra is given for the two samples from the same person. The two samples show qualitatively and quantitatively very similar spectra, while the differences between samples from different persons are visibly larger. This shows that measurements of whole hair strands give good reproducibility and make ellipsometry a suitable method for large-scale screening of hair samples.

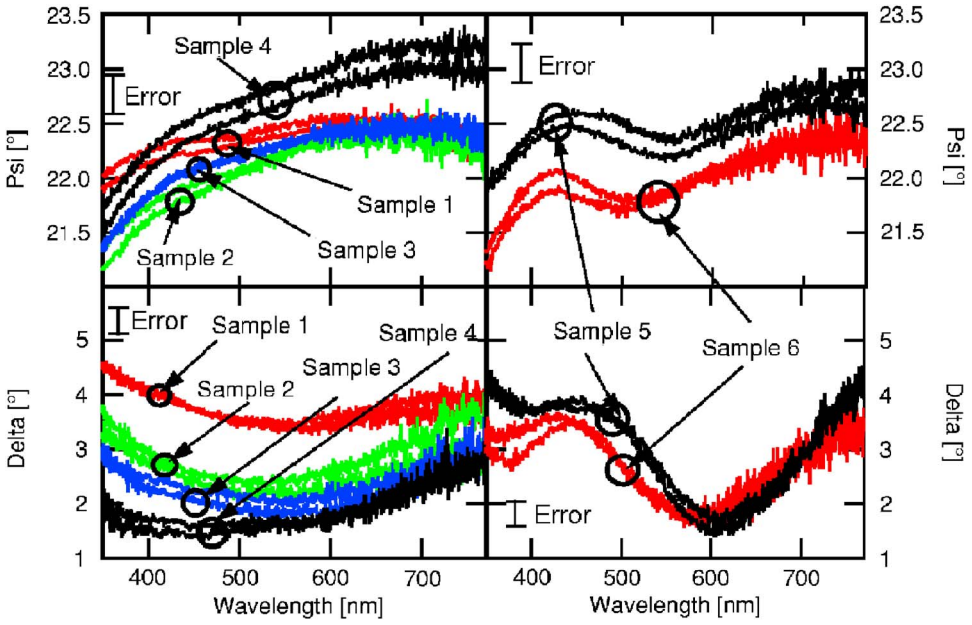

Fig. 3 Measurement of Ψ and Δ on strands of human hair from single persons. Left column: measurements on darker hair types. Right column: measurements on brighter hair types. For each person, two samples were measured, marked by equal color and the circles.

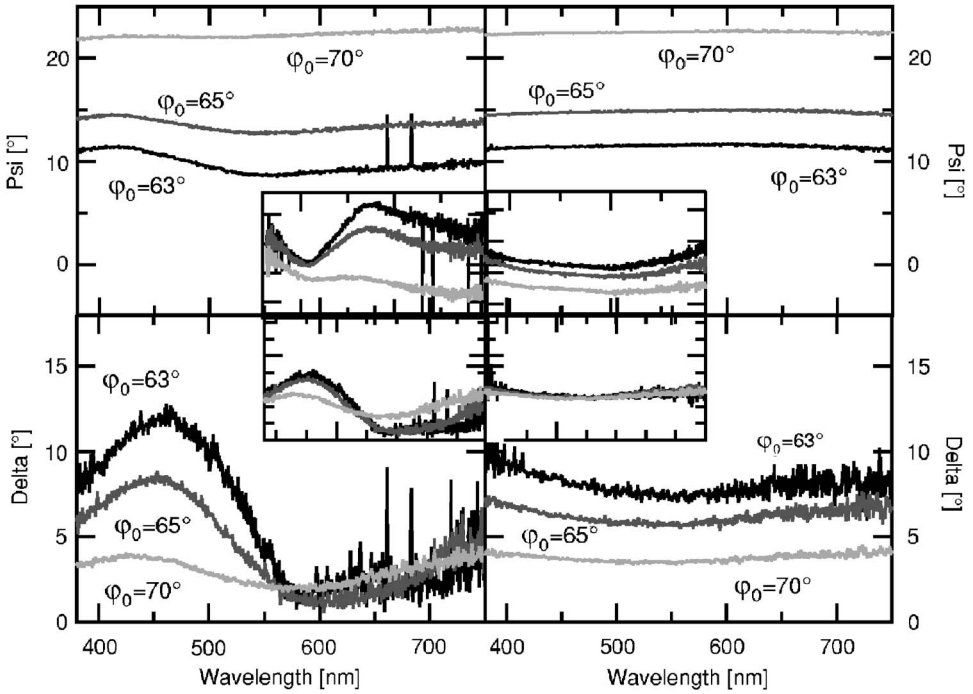

Fig. 4 Ψ-Δ spectra for two hair fiber bundles at different angles of incidence ϕ_0. Left: sample 6. Right: sample 1. The upper insets are the refractive index in the same wavelength range with a *y*-axis scaling from 1.38 to 1.48. The lower insets are the absorption coefficient *k* in the same wavelength range with a *y* axis scaling from 0 to 0.15. The complex refractive indices were computed assuming the bulk model from Eq. (2).

The measurements of the hair strands show two basic classes of spectra. These can be distinguished by their spectral features in Ψ and Δ. While four of the spectra show a mostly flat signal in both parameters with only small changes toward the UV and near-infrared (NIR) region of the spectrum, two of the spectra show a prominent peak in both parameters in the wavelength range from 400 to 600 nm.

The best differentiation of the samples is given in a wavelength range from roughly 400 to 600 nm. For larger wavelengths, the spectra become more similar, while at the same time the signal-to-noise ratio of the measurements becomes worse. For smaller wavelengths, the spectra show similar trends with decreasing values of Ψ and increasing values of Δ.

In none of the measurements are zero crossings in Δ visible. This is due to the averaging over a large collection of hairs with differing surface roughness, which can be modeled as a separate roughness layer. Both the position of a zero crossing and the strength of the oscillation will therefore change for different hairs with different thicknesses and air inclusions of the roughness layer, resulting in the average seen in the spectra. Hence, from these measurements alone it cannot be decided whether the samples can be modeled by a bulk system or not. This distinction can be made, however, by comparing measurements performed at different angles of incidence.

For the different samples, several measurements at three different angles of incidence ϕ_0=63, 65, and 70 deg were performed. Representative measurements for two samples are shown in Fig. 4.

The insets in Fig. 4 show complex refractive indices computed from the measurements, while assuming that the sample can be adequately described by the bulk model from Eq. (2). If the samples were indeed bulk systems, these converted values for the complex refractive indices should fall together, since a change in the angle of incidence does not change the sample properties. However, this is clearly not the case, which proves that the samples may not be modeled by a bulk system and are indeed layered systems. The measurements at different angles of incidence can be used, however, to model the structural and optical parameters of the hair.

4 Modeling

In the following, we present a simple dielectric model for human hair. The model is based on a representation of the major layers of the hair as isotropic, homogeneous layers.[5] The interfaces with their surface roughnesses between the cuticle and the ambient air as well as the cuticle and the cortex were modeled by additional roughness layers with complex refractive indices given by an effective medium approximation of the two adjacent media according to Eq. (5): The substructure of the cuticle is neglected in this model. The model is shown schematically in Fig. 5.

In the model, the cuticle layer below the cortex is omitted. Comparisons of fits with and without this lower layer, however, show that the influence on the calculated spectrum can be neglected.

Using this model, the multiangle measurements on hair strands as shown in Fig. 4 were fitted. All three measurements at different angles of incidence were fitted simultaneously by numerically minimizing the overall sum of the squares of all spectra using the differential evolution algorithm.[7] The complex refractive index of the cortex and the cuticle were as-

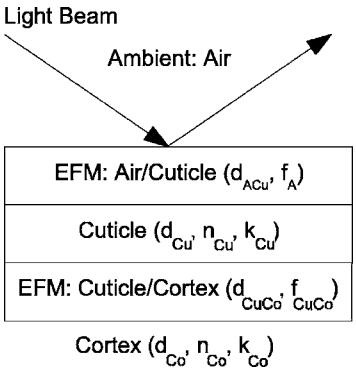

Fig. 5 Schematic representation of the dielectric layer model for human hair. d_{ACu}: thickness interface air/cuticle; f_A: effective medium ratio cuticle/air; d_{Cu}: thickness cuticle; n_{Cu}, k_{Cu}: refractive index and absorption coefficient cuticle; d_{CuCo}: thickness interface cuticle/cortex; f_{CuCo}: effective medium ratio cortex/cuticle; and n_{Co}, k_{Co}: refractive index and absorption coefficient cortex.

sumed to be constant over the whole wavelength range. Figure 6 shows the original measurements, together with the fits, represented by the dotted lines.

It can be seen that the overall shape of the data is well described by the model. In particular, the appearance of the peak structure in the range 400 to 600 nm can be reproduced by the fit.

The structural and optical parameters of the cuticle surface roughness derived from the fit of the model to the measurements are given in Table 1. The thickness of the surface roughness has values from about 270 to 360 nm, and is therefore consistent with estimates of the average edge thickness of one cuticle cell of about 350 to 500 nm.[1,2] The derived complex refractive index is in agreement with previously published values for human nails, a biologically and chemically related material.[6]

The most prominent differences between the two classes of spectra are the structural parameters of the roughness of the air/cuticle interface d_{ACu} and f_A. For the spectra with a mostly flat signal, both parameters are smaller than for the samples

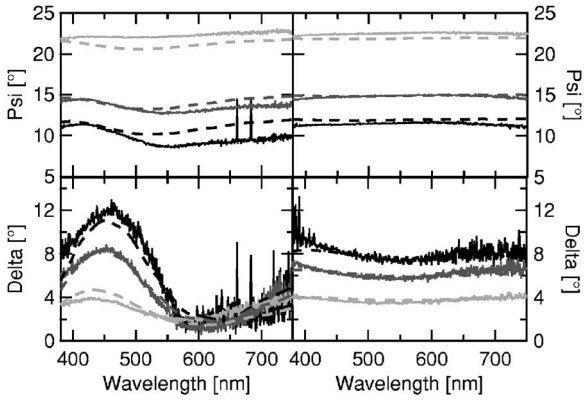

Fig. 6 Measured and calculated spectra of two strands of hair in a multiangle fit with ϕ_0=63, 65, and 70 deg. Full lines: measured spectra; dashed lines: calculated spectra given by the model shown in Fig. 5. The left column shows spectra of a European blond sample, while the right column shows spectra of a European black sample.

Table 1 Structural and optical parameters of the cuticle surface roughness layer, calculated by fits to $\Psi-\Delta$ measurements on human hair strands.

Sample	1	2	3	4	5	6
d_{ACu} [nm]	304	299.5	308.7	273.7	359.7	327.5
f_A [%]	0.6	0.1	0.8	2.2	5.7	4.7
n_{Cu}	1.45	1.46	1.47	1.46	1.5	1.50
k_{Cu}	0.055	0.043	0.04	0.039	0.056	0.047

showing the peak structure in the range 400 to 600 nm. Also, the refractive index n_{Cu} of the cuticle layer is smaller for hair types with a flat spectrum.

Figure 7 shows exemplary Δ spectra calculated with different structural and optical parameters of the surface roughness layer given by the cuticle/air interface. While changes in the thickness and air content of the roughness layer result in changes in the shape of the spectra, a change in the absorption coefficient k results in an offset of the calculated spectrum.

In contrast, the structural and optical parameters of the layers below the surface roughness do not influence the calculated spectra strongly, as can be seen by comparing spectra with different parameters for the underlying layers. As an example, Fig. 8 shows the calculated spectrum for sample 6 for two different thicknesses of the cuticle d_{Cu}=1.72 μm and 1.0 μm. The differences between the two calculated spectra

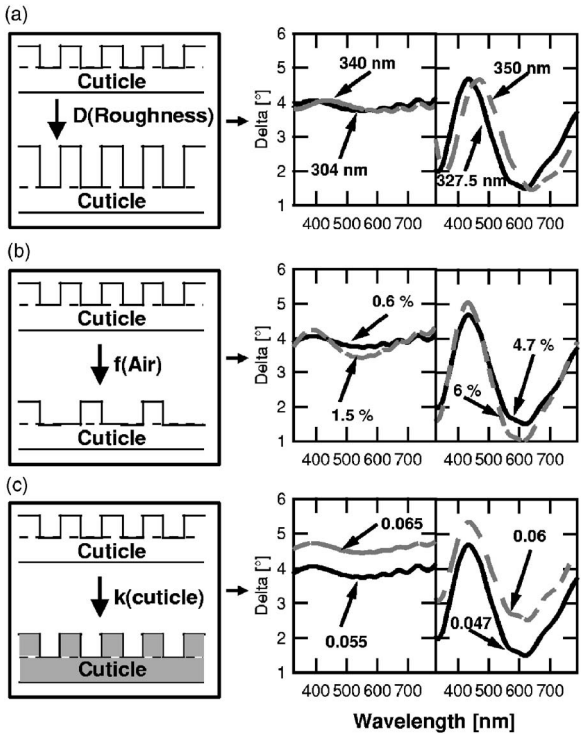

Fig. 7 Δ spectra for the two classes caused by changing structural and optical parameters of the cuticle/air interface. (a) Change in the thickness of the roughness layer. (b) Change in the air content of the roughness layer. (c) Change in the absorption coefficient k of the cuticle.

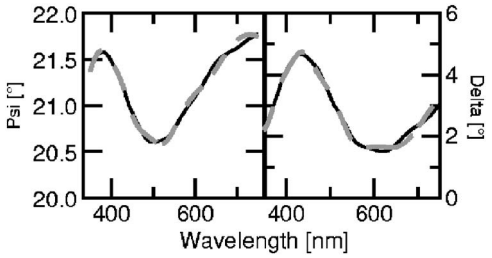

Fig. 8 Calculated Ψ-Δ spectra according to the dielectric model of Fig. 5 at $\phi_0=70$ deg with different cuticle thickness d_{Cu}. Full lines: $d_{Cu}=1.72$ μm; dashed lines: $d_{Cu}=1.0$ μm.

are small as a consequence of the weak dependence of the model on these parameters. In particular, the largest differences appear in the wavelength range above 600 nm, where the measurements show a worse signal-to-noise ratio. These findings indicate that the ellipsometric measurements are not influenced by optical and structural parameters of deeper embedded tissues like the cortex, and are rather dominated by the effective medium consisting of the cuticle and air describing the surface roughness properties of the sample.

Differences between the measured and calculated spectra can be caused by the strong assumption of a constant dispersion for both the cuticle and cortex. Also, an optical anisotropy with different optical parameters along the surface normal and in the surface plane may exist. This results in small changes in the calculated spectrum, since the light component perpendicular to the plane and the in-plane component are scattered slightly differently. Finally, the model does not account for contamination of the surface by other substances, like fat, that can be expected on a natural material like hair.

5 Conclusions

This work shows that ellipsometry is a useful tool to investigate the optical and structural parameters of biological systems with high sensitivity to surface effects. In particular, we show measurements of the ellipsometric parameters Ψ and Δ of human hair. Measurements are performed on single hairs with the hair oriented parallel and perpendicular to the plane of incidence, as well as on hair strands with the hairs oriented parallel to the plane of incidence.

The measurements on single hairs show clear signatures of a layered system and a strong optical anisotropy between the two orientations. The measurements show a strong dependence on the local properties of the sample, as shown by a large variation in the measurements of different positions along a single hair. This strong dependence is due to the differences in chemical composition and especially the local morphology, in particular the cuticle surface roughness.

To allow for measurements of a large collection of hairs in a short time, a setup for measuring whole hair strands is built. Due to limitations on the sample size and the currently used light source, only measurements in parallel orientation are possible.

Spectra of six different hair types from single persons were taken. The spectra show two different classes, with one having a mostly flat spectrum and the other showing a prominent peak in the wavelength range from 400 to 600 nm. Measurements taken under different angles of incidence $\phi_0=63$, 65, and 70 deg prove that the system under investigation has to be described using a layered model, since the conversions of the measurements to n and k using a bulk model result in different dispersions for the different angles of incidence.

A simple layer model of the hair, consisting of isotropic, homogeneous layers describing the major components of cuticle and cortex, that also allows for imperfections in the interfaces between the media, is developed. Fits of this model to the measured spectra show a good qualitative agreement. The derived structural parameters are within the expected range for human hairs.[1] The optical parameters are within the range of previously published values for nails, a closely related material.[6] The two different classes of ellipsometric spectra can be explained in this model by different surface roughness parameters of the cuticle and a differing refractive index. The dependence of the model on the parameters on parts of the hair like the cortex, which are further below the surface, is weak.

The measurements show that ellipsometry is able to resolve fine details in the surface morphology of human hairs. Together with an improved dielectric model, ellipsometry can become a useful tool for quantification of cuticle damage. The high sample throughput allows usage of ellipsometry as a screening tool for industrial applications.

Further developments of this technique include an improved experimental setup, allowing for a better signal-to-noise ratio and smaller measurement times. Both detector and light source should be optimized for maximum throughput in the visible wavelength region from about 400 to 700 nm. In addition, further automatization of the measurement process for automatic repositioning and focusing of the samples can enhance sample throughput. Moreover, further development of the dielectric model to include effects caused by optical anisotropy, the substructure of the cuticle, and surface contamination by other substances, as well as enhancements to allow for wavelength-dependent complex refractive indices, will allow for a more detailed analysis of the optical and structural parameters.

References

1. H. Zahn, "Feinbau und Chemie des Haares," *Parfümerie und Kosmetik* **65**, 3–21 (1984).
2. J. A. Swift, "Fine details on the surface of human hair," *Int. J. Cosmet. Sci.* **13**, 143–159 (1991).
3. R. F. Stamm, M. L. Garcia, and J. J. Fuchs, "The optical properties of human hair I. Fundamental considerations and goniophotometer curves," *J. Soc. Cosmet. Chem.* **28**, 601–609 (1977).
4. H. K. Bustard and R. W. Smith, "Studies of factors affecting light scattering by individual human hair fibres," *Int. J. Cosmet. Sci.* **12**, 121–133 (1990).
5. R. M. A. Azzam and N. M. Bashara, *Ellipsometry and Polarized Light*, Elsevier Science B.V., Amsterdam (1999).
6. B. Schulz, D. Chan, J. Bäckström, M. Rübhausen, K. P. Wittern, S. Wessel, R. Wepf, and S. Williams, "Hydration dynamics of human fingernails: An ellipsometric study," *Phys. Rev. E* **65**, 061913-1–061913-7 (2002).
7. R. Storn and K. Price, "Differential evolution—A simple and efficient heuristic for global optimization over continuous spaces," *J. Global Optim.* **11**, 341–359 (1997).